Heavy Quarkonium Production in Deep Inelastic Scattering From NRQCD Framework

Student: Maddox Spinelli[1]
Mentor: Farid Salazar[1]
[1]Institute for Nuclear Theory, University of Washington, Seattle, WA 98195, USA

September 9, 2024

Abstract

In this report, we work towards computing the cross-section for heavy quarkonium production in high-energy electron-proton collisions. Our methods decompose the process into an independent leptonic process and hadronic process that utilizes the non-relativistic QCD factorization formalism and includes octet contributions from S and P wave states. We compute the short distance coefficients for the production of the heavy quark pair to leading order using QCD with collinear factorization. These results pave the way for future calculations for quarkonium production in electron-nucleus collisions at small-x within the Color Glass Condensate formalism. This work contributes towards planned experiments at the future Electron-Ion Collider.

Contents

1 Introduction and Background

1.1 Introduction

One of the most pressing matters in current particle theory is resolving the internal structures of protons, neutrons, and atomic nuclei. It is a priority of the future US Electron-Ion Collider (EIC) which seeks to reveal proton and nuclei anatomies at novel precision levels [1]. Specifically, quarkonium production in Deep Inelastic Scattering (DIS) is a potential gateway into these mysteries. In this report, we discuss the production of J/Ψ particles, a type of heavy quarkonium comprised of a charm-anticharm pair, in proton DIS, and outline its relevance in probing the internal structure of protons. This project closely follows the methods used in [2] and [3]. In the future, we will extend these studies to examine nuclear DIS within the Color Glass Condensate formalism.

1.2 Background

Deep inelastic scattering is a process in which a high energy electron and a hadron scatter [4]. By observing the kinematics of the products, one is able to discern the quark-gluon structure of the hadron in the form of a one-dimensional Parton Distribution Function (PDF) or a three-dimensional Transverse Momentum-dependent parton distribution function (TMD), depending on the quantities being measured. A PDF contains information on the probability of finding a parton f inside a hadron carrying a momentum fraction x of the hadron's momentum. Once determined, PDFs are universal and can be applied to all processes involving the hadron. TMDs, on the other hand, are specific to a process, but encode more information on the motion of internal partons [5]. In this report, we restrict my focus to PDFs, but future work will explore TMD formalism and subsequently, the Color Glass Condensate [6].

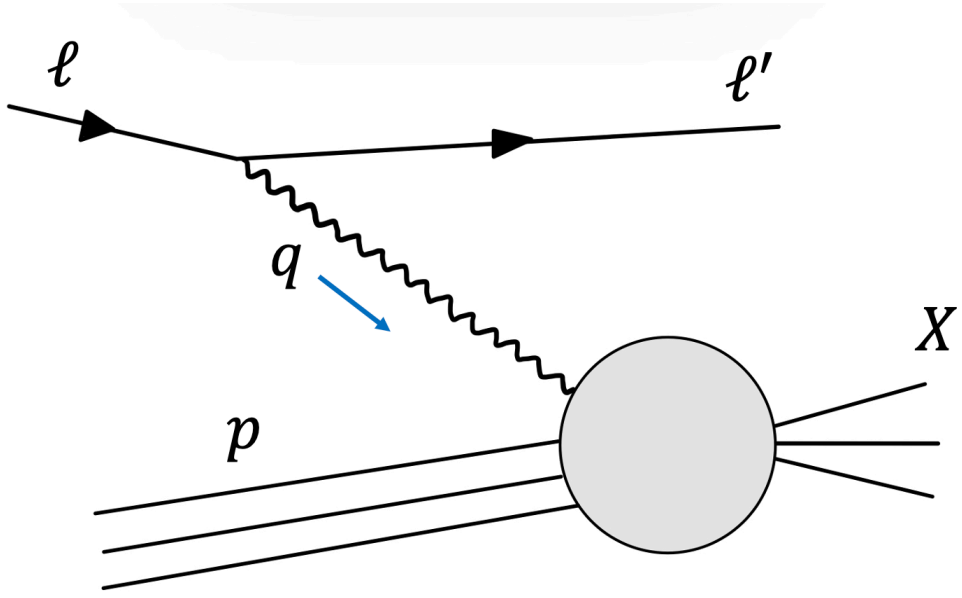

Figure 1: Schematic representation of deep inelastic scattering

The PDF of a proton has already been experimentally determined by H1 and the ZEUS collaboration [7]. Their result reveals that at large-Bjorken-x, or equivalently at low energies, we find an approximately 2:1 probability of finding an up quark to down quark, as is typically taught in undergraduate particle theory courses (parton model). However, at small Bjorken-x, or high energies ($x \sim Q^2/s$, where s is the center of mass energy squared of the collision, and Q^2 is the virtuality or resolution of the probe), the structure of a proton becomes more complex. In the high energy limit, the gluon density rises and dominates the partonic content of the hadron. We implement collinear factorization to simplify the process by computing a weighted average over each internal parton f carrying momentum fraction x in the hadron h, according to (1):

$$\sigma^{\gamma^* h \to X} = \sum_f \int dx \, \mathrm{PDF}_{f/h}(x) \cdot \sigma^{\gamma^* f \to X} \tag{1}$$

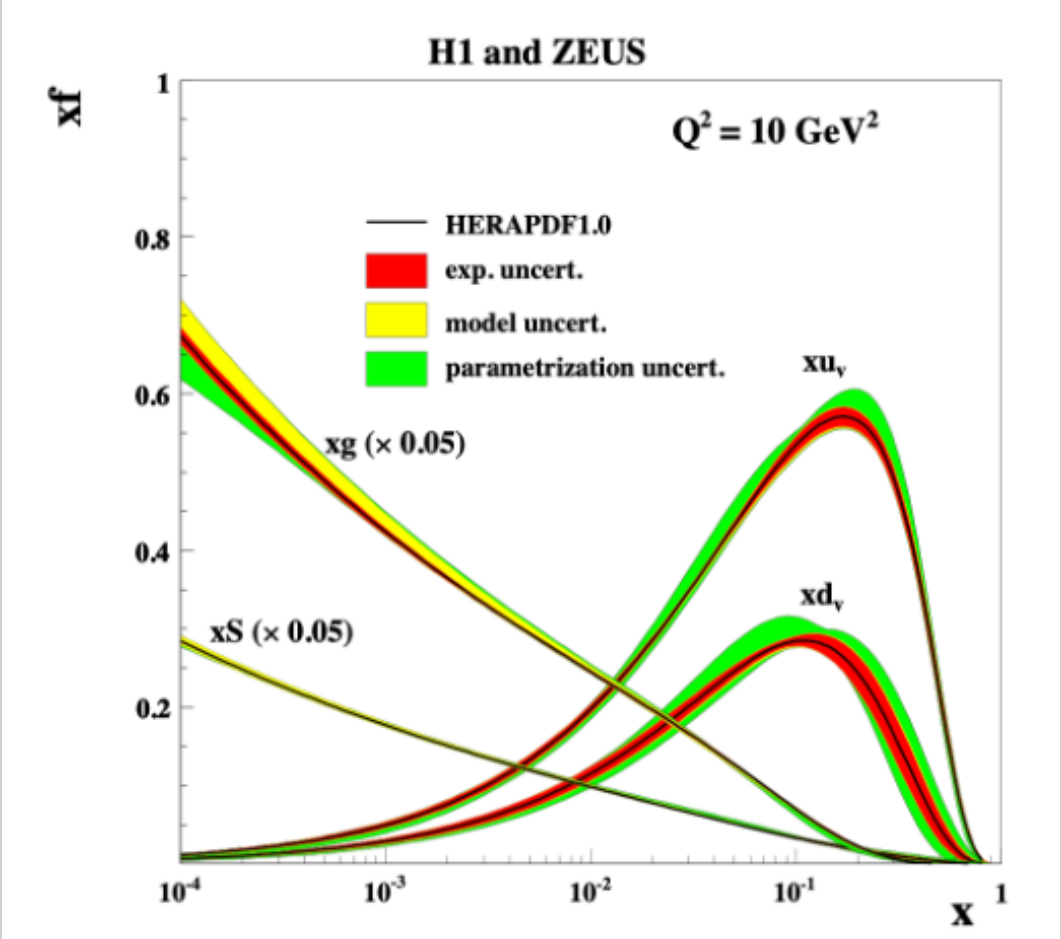

Figure 2: Parton Distribution Function (PDF) of a proton measured by H1 and ZEUS [7]

1.3 Theoretical Framework

In this report, we decompose the computation of J/Ψ production in DIS into 3 independent subprocesses, which are computed using Quantum Electrodynamics (QED), Quantum Chromodynamics (QCD), and a Non-Relativistic QCD (NRQCD) effective field theory. We follow the work in [2] to factorize any DIS process into a purely leptonic process and a hadronic process, which can

subsequently be evaluated independently. The leptonic process is simply an electron emitting a photon and scattering, and is universal in all DIS processes, simplifying our focus to the hadronic process of a hadron and virtual photon scattering. Then, using collinear factorization, we can approximate the hadronic process as the interaction of a virtual photon and a gluon. The leading order hadronic process to produce J/Ψ then becomes

$$\gamma^* g \to c\bar{c} \tag{2}$$

which we compute using QCD Feynman Rules.

Next, we employ NRQCD to to compute $c\bar{c} \to J/\Psi$. In NRQCD, we utilize an expansion of v/c to factorize complex calculations into perturbative short-distance coefficients, and non-perturbative long-distance matrix elements (LDMEs). The short-distance coefficients can be easily obtained by projecting the $c\bar{c}$ pair onto specific quantum states κ, and the LDMEs are process-independent and obtained experimentally.

2 Results

2.1 Kinematic Variables

Table 1: Kinematic variables

P (P')	incoming (outgoing) proton four-momentum
ℓ (ℓ')	incoming (outgoing) electron four-momentum
$q = \ell - \ell'$	virtual photon momentum
p_1 (p_2)	charm (anticharm) quark four-momentum
$k_g = p_1 + p_2 - q$	gluon momentum
$k = p_1 + p_2$	produced quarkonium four-momentum
$p = \frac{1}{2}(p_1 - p_2)$	half the relative four-momentum of the quarks
$m^2 = p_1^2 = p_2^2$	charm quark invariant mass squared
$M^2 = k^2$	invariant mass squared of produced quarkonium H
$Q^2 = -q^2$	virtuality of exchanged photon
$y = \frac{P\cdot q}{P\cdot \ell}$	inelasticity: in $\vec{P} = 0$ frame the fraction of ℓ carried by the virtual photon
$z = \frac{p_1^-}{q^-}$	light-cone longitudinal momentum fraction of charm quark ($1 - z$ for antiquark)

In this report we work with light-cone coordinates:

$$a^{\pm} = \frac{1}{\sqrt{2}}\left(a^0 \pm a^3\right) \tag{3}$$

We write four-vectors as

$$a^{\mu} = \left(a^+, a^-, \boldsymbol{a}_{\perp}\right) \tag{4}$$

where $\boldsymbol{a}_\perp = (a^1, a^2)$. We use the following canonical light-cone vectors:

$$\begin{aligned} n^\mu &= (1, 0, \mathbf{0}_\perp) \\ \bar{n}^\mu &= (0, 1, \mathbf{0}_\perp) \end{aligned} \tag{5}$$

We ignore the mass of the electron and the mass of the proton.

We work in a frame where:

$$q^\mu = \left(-\frac{Q^2}{2q^-}, q^-, \mathbf{0}_\perp\right) \tag{6}$$

$$P^\mu = (P^+, 0, \mathbf{0}_\perp) \tag{7}$$

$$k_g^\mu = (k_g^+, 0, \mathbf{0}_\perp)\,, \tag{8}$$

where we have assumed that the gluon only carries longitudinal momentum since we will be using collinear factorization.

The quarks then have 4-momenta:

$$\begin{aligned} p_1^\mu &= \left(\frac{\boldsymbol{p}_\perp^2 + m^2}{2zq^-}, zq^-, \boldsymbol{p}_\perp\right) \\ p_2^\mu &= \left(\frac{\boldsymbol{p}_\perp^2 + m^2}{2(1-z)q^-}, (1-z)q^-, -\boldsymbol{p}_\perp\right) \end{aligned} \tag{9}$$

where $\boldsymbol{p}_\perp = (p_\perp \cos(\phi_p), p_\perp \sin(\phi_p))$, and the incoming electron has 4-momentum:

$$\ell^\mu = \left(\frac{\boldsymbol{\ell}_\perp^2}{2\ell^-}, \ell^-, \boldsymbol{\ell}_\perp\right) \tag{10}$$

where $\boldsymbol{\ell}_\perp = (\ell_\perp \cos(\phi_\ell), \ell_\perp \sin(\phi_\ell))$. In this frame, the photon polarization vectors (in light-cone gauge $A \cdot n = A^- = 0$) read:

$$\begin{aligned} \varepsilon^\mu(q, \lambda = 0) &= \left(\frac{Q}{q^-}, 0, \mathbf{0}_\perp\right) \\ \varepsilon^\mu(q, \lambda = \pm 1) &= \left(0, 0, \boldsymbol{\epsilon}_\perp^\lambda\right) \end{aligned} \tag{11}$$

where

$$\boldsymbol{\epsilon}_\perp^\lambda = \frac{1}{\sqrt{2}}(1, i\lambda) \tag{12}$$

2.2 Lepton-hadron decomposition

The amplitude for a general DIS process involving the collision of an electron and proton can be decomposed into a leptonic and a hadronic component, using the regular Feynman Rules:

$$\mathcal{M}^{ep\to e+X} = \bar{u}(\ell')(-ie\gamma_\mu)u(\ell)\frac{\Pi^{\mu\nu}(q)}{q^2}\mathcal{M}_\nu^{\gamma^* p\to X} \tag{13}$$

where $\mathcal{M}_\nu^{\gamma^* p\to X}$ is the amplitude[1] for the scattering of a virtual photon with a proton producing a final state X, and $\Pi_{\mu\nu}(q)$ denotes the photon polarization tensor which satisfies the completeness relation:

[1] where we amputated the polarization vector of the photon

$$\Pi_{\mu\nu}(q) = \sum_{\lambda} (-1)^{\lambda+1} \cdot \varepsilon^*_\mu(\lambda, q) \cdot \varepsilon_\nu(\lambda, q) \tag{14}$$

After averaging and summing over the spin of the incoming and outgoing electrons respectively, the amplitude squared can be written as

$$\frac{1}{2} \sum_{\text{spin}} \left| \mathcal{M}^{ep\to e+X} \right|^2 = X_{\mu\nu} L^{\mu\nu} \tag{15}$$

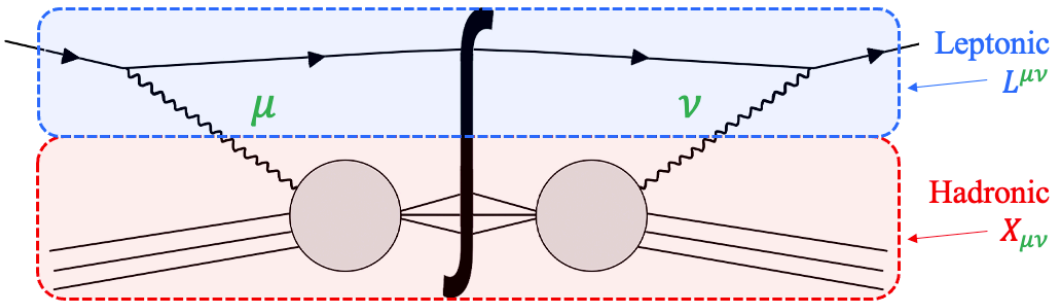

Figure 3: Schematic of lepton-hadron tensor decomposition.

The process-independent leptonic tensor is

$$L^{\mu\nu} = \frac{e^2}{2Q^4} \text{Tr}\left[\not{\ell} \gamma^\mu \not{\ell}' \gamma^\nu\right] \tag{16}$$

while the process-specific hadronic tensor is

$$X_{\mu\nu} = \overline{\sum} \left(\mathcal{M}^{\gamma^* p\to X}_\mu\right)^* \mathcal{M}^{\gamma^* p\to X}_\nu \tag{17}$$

where $\overline{\sum}$ denotes appropriate sum/average over quantum numbers.

We can reduce the number of components to sum over in Eq. (15) from 16 in the usual Minkowski basis to 9 by reformulating the tensors in the polarization basis of the virtual photon using Eq. (14). The photon polarization (in light-cone gauge $A \cdot n = A^- = 0$) is

$$\Pi^{\mu\nu} = -g^{\mu\nu} + \frac{n^\mu q^\nu + q^\mu n^\nu}{q.n} \tag{18}$$

We thus can write Eq. (15) as

$$\left| \mathcal{M}^{ep\to e+X} \right|^2 = \sum_{\lambda,\bar{\lambda}} X_{\lambda\bar{\lambda}} L_{\lambda\bar{\lambda}} \tag{19}$$

where $\bar{\lambda}$ is the polarization of the conjugate virtual photon and

$$\begin{aligned} L_{\lambda\bar{\lambda}} &= (-1)^{\lambda+\bar{\lambda}} \varepsilon_\mu(q,\lambda) \varepsilon^*_\nu(q,\bar{\lambda}) L^{\mu\nu} \\ X_{\lambda\bar{\lambda}} &= \varepsilon^*_\mu(q,\lambda) \varepsilon_\nu(q,\bar{\lambda}) X^{\mu\nu} \end{aligned} \tag{20}$$

We've now reduced the components to only the physical ones. Substituting in the original tensors, we have:

$$L_{\lambda\bar{\lambda}} = (-1)^{\lambda+\bar{\lambda}} \frac{e^2}{2Q^4} \varepsilon_\mu(q,\lambda)\varepsilon^*_\nu(q,\bar{\lambda}) \mathrm{Tr}\left[\not{\ell}\gamma^\mu \not{\ell}'\gamma^\nu\right] \tag{21}$$

$$X_{\lambda\bar{\lambda}} = \overline{\sum} \left(\mathcal{M}^{\gamma^* p\to X}_{\lambda}\right)^* \mathcal{M}^{\gamma^* p\to X}_{\bar{\lambda}} \tag{22}$$

where

$$\mathcal{M}^{\gamma^* p\to X}_{\bar{\lambda}} = \varepsilon_\mu(q,\lambda)\mathcal{M}^{\gamma^* p\to X}_{\mu} \tag{23}$$

is the amplitude for the scattering of a virtual photon with polarization λ with a proton.

In the next section, we will show that the leptonic tensor has the form:

$$L_{\lambda\bar{\lambda}} = \widetilde{L}_{\lambda\bar{\lambda}}\, e^{i(\lambda-\bar{\lambda})\phi_\ell} \tag{24}$$

where ϕ_ℓ is the azimuthal angle of the electron, and $\widetilde{L}_{\lambda\bar{\lambda}}$ are independent of ϕ_ℓ. Similarly, the hadronic tensor for single-inclusive particle production will have the form

$$X_{\lambda\bar{\lambda}} = \widetilde{X}_{\lambda\bar{\lambda}}\, e^{-i(\lambda-\bar{\lambda})\phi_k} \tag{25}$$

where ϕ_k is the azimuthal angle of the produced particle, and $\widetilde{X}_{\lambda\bar{\lambda}}$ are independent of ϕ_k. Combining these results we find:

$$\left|\mathcal{M}^{ep\to e+X}\right|^2 = (L_{00}X_{00} + 2L_{11}X_{11}) + 4L_{10}X_{10}\cos(\phi_\ell - \phi_k) + 2L_{-11}X_{-11}\cos(2(\phi_\ell - \phi_k))\,. \tag{26}$$

To obtain this result we use the following properties of the leptonic and hadronic tensor components:

$$\widetilde{L}_{\lambda\bar{\lambda}} = \widetilde{L}_{\bar{\lambda}\lambda} = \widetilde{L}_{-\lambda-\bar{\lambda}} \tag{27}$$

$$\widetilde{X}_{\lambda\bar{\lambda}} = \widetilde{X}_{\bar{\lambda}\lambda} = \widetilde{X}_{-\lambda-\bar{\lambda}}\,, \tag{28}$$

which are satisfied by the process under consideration and will be shown explicitly in the next sections.

2.3 Leptonic Process

Evaluating Eq. (21) using the explicit forms of the photon polarization vectors yields:

$$L_{\lambda\bar{\lambda}} = \widetilde{L}_{\lambda\bar{\lambda}}\, e^{i(\lambda-\bar{\lambda})\phi_\ell} \tag{29}$$

where

$$\begin{aligned}
\widetilde{L}_{00} &= \frac{4e^2(1-y)}{y^2Q^2} \\
\widetilde{L}_{\pm1\pm1} &= \frac{e^2\left[1+(1-y)^2\right]}{y^2Q^2}, \\
\widetilde{L}_{\pm1\mp1} &= \frac{2e^2(1-y)}{y^2Q^2}, \\
\widetilde{L}_{0\pm1} = \widetilde{L}_{\pm10} &= -\frac{e^2\sqrt{2-2y}(2-y)}{y^2Q^2}
\end{aligned} \tag{30}$$

Or in matrix form:

$$L_{\lambda\bar{\lambda}} = \frac{e^2}{y^2Q^2}\begin{bmatrix} [1+(1-y)^2] & 2(1-y)e^{2i\phi_\ell} & -\sqrt{2-2y}\,(2-y)e^{i\phi_\ell} \\ 2(1-y)e^{-2i\phi_\ell} & [1+(1-y)^2] & -\sqrt{2-2y}\,(2-y)e^{-i\phi_\ell} \\ -\sqrt{2-2y}\,(2-y)e^{-i\phi_\ell} & -\sqrt{2-2y}\,(2-y)e^{i\phi_\ell} & 4(1-y) \end{bmatrix} \tag{31}$$

Notice that the diagonal elements of $L_{\lambda\bar{\lambda}}$ correspond to the scattering of a virtual photon with polarization λ with an electron, while the off-diagonal matrix elements correspond to the inference between different photon polarizations in the amplitude and conjugate amplitude. The result in Eq. (31) can be found in [2] [2].

2.4 Hadronic Process in collinear factorization

It is helpful to consider the hadronic process at the level of the cross-section as opposed to the amplitude for now. For the moment we assume the virtual photon γ^* with polarization λ interacts with a parton f inside the proton p, and that each parton moves collinearly to the proton carrying a fraction x of its momentum. $\mathrm{PDF}_f(x)$ is the probability density to find a parton f with a given momentum fraction x during the interaction. The cross-section in (semi-inclusive) proton DIS can then be computed in collinear factorization as

$$\begin{aligned} &\sigma\left(\gamma^*(\lambda) + p(P) \to \sum_{i=1}^{n} \mathbb{p}_i(p_i) + X\right) \\ &= \sum_f \int \mathrm{d}x\ \mathrm{PDF}_{f/p}(x)\sigma\left(\gamma^*(\lambda) + f(xP) \to \sum_{i=1}^{n} \mathbb{p}_i(p_i)\right) \end{aligned} \tag{32}$$

where $\mathbb{p}_i$ denotes the particles measured, while X denotes the remnants of the shattered proton which are not measured.

We have reduced the problem to evaluating the partonic process

$$\gamma^*(q) + f(xP) \to \sum_{i=1}^{n} \mathbb{p}_i(p_i) \tag{33}$$

which involves the photon, the parton, and the measured particles in the final state.

[2] Note that we have a different normalization than [2] since we absorbed the factor $1/Q^4$ in our definition of the lepton tensor.

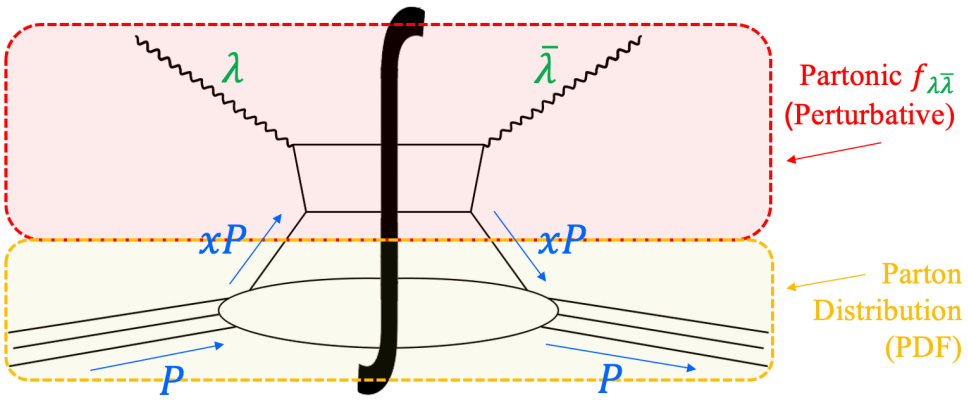

Figure 4: collinear factorization of a photon-nucleus collision

We can cast the differential cross-section for single-inclusive particle production in DIS as

$$\frac{\mathrm{d}\sigma\left(p(P)+e(\ell)\to H(k)+e(\ell')+X\right)}{\mathrm{d}y\mathrm{d}Q^2\mathrm{d}\phi_{\ell k}}=\frac{y}{4(2\pi)^3}\sum_f \mathrm{PDF}_{f/h}(x_f)\frac{\pi}{(Q^2+M^2)^2}\left|\mathcal{M}^{e+f\to e+H+X}\right|^2 \tag{34}$$

where $\phi_{\ell k}=\phi_\ell-\phi_k$ is the relative azimuthal angle between the electron and the produced particle, $M^2=k^2$ is the invariant mass squared of the produced particle H, and $X_\kappa^{\lambda\bar{\lambda}}$ corresponds to the production amplitude squared (averaged/summed over quantum numbers) with different polarization in the amplitude and conjugate amplitude. The density matrix $X^{\lambda\bar{\lambda}}$ will be computed in the next subsection.

2.5 Partonic Process

We begin by calculating the amplitude square for open heavy-quark pair production. We then present a calculation for quarkonium production using NRQCD.

2.5.1 Open heavy-quark pair production

At leading order in α_s, the heavy-quark pair is produced via photon gluon fusion:[3]

$$\gamma^*(\lambda)+g(k_g)\to c(p_1)+\bar{c}(p_2) \tag{35}$$

where c and $\bar{c}$ are the charm/anticharm quark pair that will later combine to form J/ψ. The amplitude for this process is given by

$$\left(\mathcal{M}^{\gamma^* g\to c\bar{c}}\right)_{s\bar{s},i\bar{i}}^{\lambda\lambda_g a}=\varepsilon_\mu(q,\lambda)\varepsilon_\alpha(k_g,\lambda_g)\bar{u}(p_1,s)\Gamma^{\mu\alpha}v(p_2,\bar{s})t^a_{i\bar{i}} \tag{36}$$

where the polarizations of the virtual photon and gluon are denoted by λ and λ_g, while $s/\bar{s}$ and $i/\bar{i}$ denote the spin and color index of the quark/anti-quark respectively.[4] $\Gamma^{\mu\alpha}$ contains the appropriate gamma matrices:

$$\Gamma^{\mu\alpha}=ieg\left(\frac{\gamma^\mu(\not{p}_1-\not{q}+m)\gamma^\alpha}{(p_1-q)^2-m^2}+\frac{\gamma^\alpha(\not{q}-\not{p}_2+m)\gamma^\mu}{(q-p_2)^2-m^2}\right) \tag{37}$$

[3]The quark initiated channel is next-to-leading order.

[4]Within the scope of this report the gluon polarization is averaged out.

After averaging the incoming gluon color and polarization and summing the outgoing quark and antiquark spins and colors, the amplitude squared becomes

$$X_{\lambda\bar{\lambda}}^{\gamma^* g\to c\bar{c}} = \frac{1}{2}\frac{1}{N_c^2-1}\sum_{s,\bar{s},\lambda_g,a}\left(\mathcal{M}^{\gamma^* g\to q\bar{q}}\right)^{*\lambda\lambda_g a}_{s\bar{s},i\bar{i}}\left(\mathcal{M}^{\gamma^* g\to q\bar{q}}\right)^{\bar{\lambda}\lambda_g a}_{s\bar{s},i\bar{i}}$$
$$= \frac{1}{4}\varepsilon_\mu(q,\lambda)\varepsilon^*_\nu(q,\bar{\lambda})\mathrm{Tr}\left[\not{p}_1\Gamma^{\mu\alpha}\not{p}_2\overline{\Gamma}^{\nu\beta}\right](-g_{\alpha\beta}) \tag{38}$$

where we we chose to work in Feynman gauge for the gluon field.

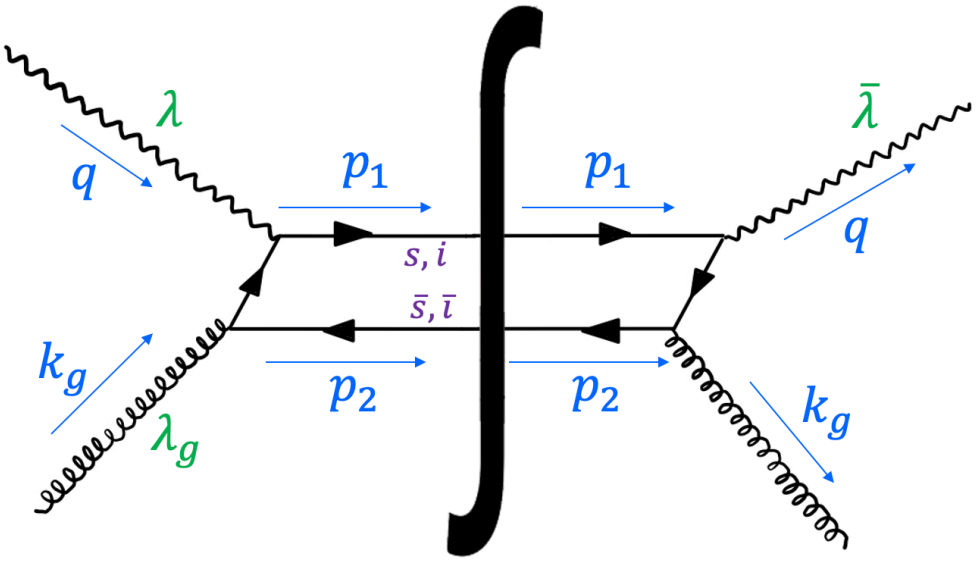

Figure 5: Photon-gluon fusion process to produce a pair of quarks.

Carrying out the contractions in our chosen frame, we find that the hadronic tensor under collinear factorization takes the form:

$$X_{\lambda\bar{\lambda}}^{\gamma^* g\to c\bar{c}} = \widetilde{X}_{\lambda\bar{\lambda}}\, e^{-i(\lambda-\bar{\lambda})\phi_p} \tag{39}$$

where

$$\begin{aligned}
\widetilde{X}_{00} &= \frac{8e^2g^2p_\perp^2\omega}{(p_\perp^2+\omega)^2},\\
\widetilde{X}_{\pm1\pm1} &= e^2g^2\left[\frac{2m^2p_\perp^2+[z^2+(1-z)^2]\,[p_\perp^4+\omega^2]}{z(1-z)(p_\perp^2+\omega)^2}\right],\\
\widetilde{X}_{\pm1\mp1} &= \frac{4e^2g^2p_\perp^2}{(p_\perp^2+\omega)^2}\omega,\\
\widetilde{X}_{0\pm1} &= \widetilde{X}_{\pm10} = \frac{\sqrt{2}e^2g^2\,p_\perp Q(2z-1)(p_\perp^2-\omega)}{(p_\perp^2+\omega)^2}
\end{aligned} \tag{40}$$

and

$$\omega \equiv z(1-z)Q^2+m^2 \tag{41}$$

2.5.2 Quarkonium production with NRQCD

We employ Non-Relativistic QCD (NRQCD) [8] to describe the recombination of heavy quarks into a quarkonium H. First, we evaluate the short-distance coefficients, $\hat{\sigma}^\kappa$, for the production of a heavy quark pair in a given quantum state $\kappa = {}^{2S+1}L_J^{[c]}$. Each state has definite spin S, orbital angular momentum L, total angular momentum J and color state $[c]$. Next, the short-distance coefficients are weighted with non-perturbative long-distance matrix elements (LDMEs), $\langle \mathcal{O}_\kappa^H \rangle$, and summed:

$$\sigma_H = \sum_\kappa \hat{\sigma}^\kappa \langle \mathcal{O}_\kappa^H \rangle \,. \tag{42}$$

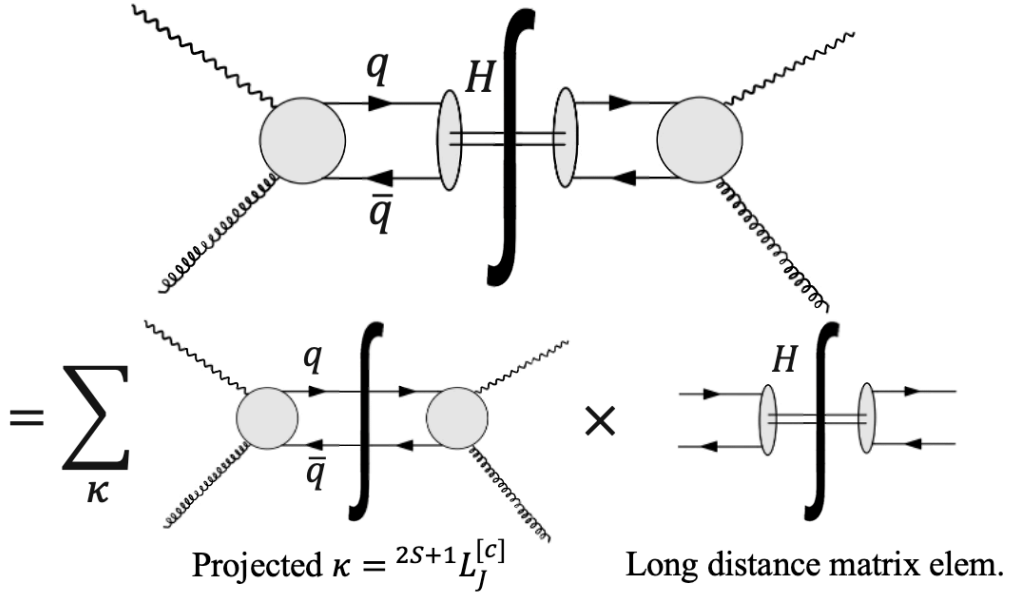

Figure 6: Schematic representation of NRQCD factorization of σ_H, Eq. (42)

To compute $\hat{\sigma}^\kappa$ we project the quark/anti-quark pair $q\bar{q}$ amplitude to the specific quantum state κ. For J/Ψ production, only three color octet states and one color singlet state contribute, so $\kappa \in \{{}^1S_0^{[8]}, {}^3S_1^{[8]}, {}^3P_J^{[8]}, {}^3S_1^{[1]}\}$ as in [9]. The amplitude for $\hat{\sigma}^\kappa$, $\mathcal{M}_{\kappa,J_z}^{\lambda\lambda_g a}(k)$, is then:

$$\begin{aligned}\mathcal{M}_{\kappa,J_z}^{\lambda\lambda_g a}(k) = \frac{1}{\sqrt{m}} \sum_{\substack{L_z,S_z \\ s,\bar{s},i,\bar{i}}} \langle LL_z; SS_z | JJ_z \rangle \left\langle \frac{1}{2}s; \frac{1}{2}\bar{s} \middle| SS_z \right\rangle \langle 3i; \bar{3}\bar{i} | (1,8c) \rangle \\ \times \begin{cases} \mathcal{M}_{s\bar{s},i\bar{i}}^{\lambda\lambda_g a}(0,k) & \text{if } \kappa \text{ is } S-\text{wave}\,, \\ \epsilon_\beta^*(L_z) \frac{\partial \mathcal{M}_{s\bar{s},i\bar{i}}^{\lambda\lambda_g a}(p,k)}{\partial p_\beta}\Big|_{p=0} & \text{if } \kappa \text{ is } P-\text{wave}\,. \end{cases}\end{aligned} \tag{43}$$

where $\mathcal{M}_{s\bar{s},i\bar{i}}^{\lambda\lambda_g a}(p,k)$ is the amplitude for $c\bar{c}$ production, as in Eq. (36), and $\epsilon_\beta(L_z)$ is the polarization vector of the quarkonium.

To compute the color projections we use the following identities:

$$\begin{aligned}\langle 3i; \bar{3}\bar{i} | 1 \rangle &= \delta^{i\bar{i}}/\sqrt{N_c} \\ \langle 3i; \bar{3}\bar{i} | 8c \rangle &= \sqrt{2} t_c^{i\bar{i}}\end{aligned} \tag{44}$$

Note that only the color octet is non-vanishing since $\mathcal{M}^{\lambda\lambda_g a}_{s\bar{s},i\bar{i}}(p,k)$ is proportional to $t^a_{i\bar{i}}$. Therefore:

$$\sum_{i,\bar{i}} \mathcal{M}^{\lambda\lambda_g a}_{s\bar{s},i\bar{i}}(p,k)\langle 3i;\overline{3i}|8c\rangle = \varepsilon_\mu(q,\lambda)\varepsilon_\alpha(k_g,\lambda_g)\bar{u}(p_1,s)\Gamma^{\mu\alpha}(p,k)v(p_2,\bar{s})\sqrt{2}\mathrm{Tr}\left[t^a t_c\right]$$

$$= \bar{u}(p_1,s)\mathcal{N}^{\lambda\lambda_g}(p,k)v(p_2,\bar{s})\frac{\delta^a_c}{\sqrt{2}} \tag{45}$$

where we've cleaned things up in the second line by writing:

$$\mathcal{N}^{\lambda\lambda_g}(p,k) \equiv \varepsilon_\mu(q,\lambda)\varepsilon_\alpha(k_g,\lambda_g)\Gamma^{\mu\alpha}(p,k) \tag{46}$$

with $\Gamma^{\mu\alpha}(p,k)$ defined in Eq. (37).

To compute the spinor projections, we first define the projector:

$$\Pi^{SS_z}(p,k) \equiv \frac{1}{\sqrt{m}}\sum_{s,\bar{s}}\left\langle \frac{1}{2}s;\frac{1}{2}\bar{s}\middle| SS_z\right\rangle v\left(\frac{k}{2}-p,\bar{s}\right)\bar{u}\left(\frac{k}{2}+p,s\right). \tag{47}$$

which enables us to express the projections as:

$$\mathcal{M}^{\lambda\lambda_g a}_{\kappa,J_z,c}(k) = \frac{\delta^a_c}{\sqrt{2}}\sum_{L_z,S_z}\langle LL_z;SS_z|JJ_z\rangle$$
$$\times\begin{cases}\mathrm{Tr}\left[\mathcal{N}^{\lambda\lambda_g}(0,k)\Pi^{SS_z}(0,k)\right] & \text{if } \kappa \text{ is } S-\text{wave}\,,\\ \epsilon^*_\beta(L_z)\frac{\partial\mathrm{Tr}\left[\mathcal{N}^{\lambda\lambda_g}(p,k)\Pi^{SS_z}(p,k)\right]}{\partial p_\beta}\Big|_{p=0} & \text{if } \kappa \text{ is } P-\text{wave}\,.\end{cases} \tag{48}$$

Next, we use the following identities

$$\Pi^{00}(p,k) = \frac{1}{\sqrt{8m^3}}\left(\frac{\not{k}}{2}-\not{p}-m\right)\gamma^5\left(\frac{\not{k}}{2}+\not{p}+m\right) \tag{49}$$

$$\Pi^{1S_z}(p,k) = \epsilon^*_\rho(S_z)\widetilde{\Pi}^{1,\rho}(p,k) \tag{50}$$

with

$$\widetilde{\Pi}^{1,\rho}(p,k) = \frac{1}{\sqrt{8m^3}}\left(\frac{\not{k}}{2}-\not{p}-m\right)\gamma^\rho\left(\frac{\not{k}}{2}+\not{p}+m\right). \tag{51}$$

The corresponding amplitude square projection for a given state κ is:

$$X^{\lambda\bar{\lambda}}_\kappa = \frac{1}{2(N_c^2-1)}\frac{1}{(2J+1)(N_c^2-1)}\sum_{\lambda_g,a,J_z,c}\mathcal{M}^{*\lambda\lambda_g a}_{\kappa,J_z,c}\mathcal{M}^{\lambda\lambda_g a}_{\kappa,J_z,c} \tag{52}$$

$$= \frac{1}{2(N_c^2-1)}\frac{1}{(2J+1)(N_c^2-1)}\sum_{\lambda_g,J_z}\mathcal{M}^{*\lambda\lambda_g}_{\kappa,J_z}\mathcal{M}^{\lambda\lambda_g}_{\kappa,J_z}\frac{1}{2}\sum_{a,c}\delta^a_c\delta^a_c \tag{53}$$

where we have factored out the color part from the amplitude in the second line. In the first line the factor $\frac{1}{2(N_c^2-1)}$ comes from averaging over the spin and color of the incoming gluon, and the factor $\frac{1}{(2J+1)(N_c^2-1)}$ comes from the degeneracy of states of the the state κ.

For the three color octets, this yields:

$$X^{\lambda\bar{\lambda}}_{{}^1S_0^{[8]}} = \frac{1}{(2J+1)(N_c^2-1)}\frac{1}{4}\sum_{\lambda_g}\left(\mathrm{Tr}\left[\mathcal{N}^{\lambda\lambda_g}(0,k)\Pi^{0S_z}(0,k)\right]\right)^*\mathrm{Tr}\left[\mathcal{N}^{\bar{\lambda}\lambda_g}(0,k)\Pi^{0S_z}(0,k)\right] \tag{54}$$

$$X^{\lambda\bar{\lambda}}_{{}^3S_1^{[8]}} = \frac{1}{(2J+1)(N_c^2-1)}\frac{1}{4}\mathbb{P}_{\rho\rho'}\sum_{\lambda_g}\left(\mathrm{Tr}\left[\mathcal{N}^{\lambda\lambda_g}(0,k)\widetilde{\Pi}^{1,\rho}(0,k)\right]\right)^*\mathrm{Tr}\left[\mathcal{N}^{\bar{\lambda}\lambda_g}(0,k)\widetilde{\Pi}^{1,\rho'}(0,k)\right] \tag{55}$$

$$\begin{aligned}X^{\lambda\bar{\lambda}}_{{}^3P_J^{[8]}} &= \frac{1}{(2J+1)(N_c^2-1)}\frac{1}{4}\sum_{J_z}\epsilon_{\beta\rho}(J,J_z)\epsilon^*_{\beta'\rho'}(J,J_z)\\ &\times\sum_{\lambda_g}\left(\frac{\partial\mathrm{Tr}\left[\mathcal{N}^{\lambda\lambda_g}(p,k)\widetilde{\Pi}^{1,\rho}(p,k)\right]}{\partial p_\beta}\Big|_{p=0}\right)^*\frac{\partial\mathrm{Tr}\left[\mathcal{N}^{\bar{\lambda}\lambda_g}(p,k)\widetilde{\Pi}^{1,\rho'}(p,k)\right]}{\partial p_{\beta'}}\Big|_{p=0}\end{aligned} \tag{56}$$

where

$$\mathbb{P}_{\rho\rho'} \equiv \sum_{J_z}\epsilon^*_\rho(J_z)\epsilon_{\rho'}(J_z) = -g_{\rho\rho'} + \frac{k_\rho k_{\rho'}}{k^2} \tag{57}$$

and

$$\epsilon^*_{\beta\rho}(J,J_z) \equiv \sum_{L_z,S_z}\langle 1L_z;1S_z|JJ_z\rangle\epsilon^*_\beta(L_z)\epsilon^*_\rho(S_z) \tag{58}$$

To compute the P-wave we employ the following identities:

$$\sum_{J_z}\epsilon^*_{\rho\mu}(0,J_z)\epsilon_{\rho'\mu'}(0,J_z) = \frac{1}{3}\mathbb{P}_{\rho\mu}\mathbb{P}_{\rho'\mu'}\,, \tag{59}$$

$$\sum_{J_z}\epsilon^*_{\rho\mu}(1,J_z)\epsilon_{\rho'\mu'}(1,J_z) = \frac{1}{2}\left(\mathbb{P}_{\rho\rho'}\mathbb{P}_{\mu\mu'} - \mathbb{P}_{\rho\mu'}\mathbb{P}_{\rho'\mu}\right)\,, \tag{60}$$

$$\sum_{J_z}\epsilon^*_{\rho\mu}(2,J_z)\epsilon_{\rho'\mu'}(2,J_z) = \frac{1}{2}\left(\mathbb{P}_{\rho\rho'}\mathbb{P}_{\mu\mu'} + \mathbb{P}_{\rho\mu'}\mathbb{P}_{\rho'\mu}\right) - \frac{1}{3}\mathbb{P}_{\rho\mu}\mathbb{P}_{\rho'\mu'}\,. \tag{61}$$

It is convenient to introduce the mass of the quarkonium $M = 2m$. The results of the hadron tensor computations are expressed in Table 2.

2.6 Differential cross section for quarkonium production

Following NRQCD we write the differential cross-section for quarkonium production in DIS as

$$\frac{\mathrm{d}\sigma\left(p(P)+e(\ell)\to H(k)+e(\ell')+X\right)}{\mathrm{d}y\mathrm{d}Q^2\mathrm{d}\phi_{\ell k}} = \sum_\kappa\frac{\mathrm{d}\hat{\sigma}_\kappa}{\mathrm{d}y\mathrm{d}Q^2\mathrm{d}\phi_{\ell k}}\langle\mathcal{O}^H_\kappa\rangle \tag{62}$$

where $\frac{\mathrm{d}\hat{\sigma}_\kappa}{\mathrm{d}y\mathrm{d}Q^2\mathrm{d}\phi_{\ell k}}$ are the short distance coefficients for quarkonium production in DIS.

We combine the results for the lepton-hadron decomposition of the amplitude squared in Eq. (26) with the elements of the lepton tensor derived in Sec. 2.3, and collinear factorization (see Eq. (34)) to find:

$$\begin{aligned}\frac{\mathrm{d}\hat{\sigma}_\kappa}{\mathrm{d}y\mathrm{d}Q^2\mathrm{d}\phi_{\ell k}} = \frac{\alpha_{\mathrm{em}}}{8\pi^2yQ^2}\Big[&4(1-y)\sigma^\kappa_{00} + \left[1+(1-y)^2\right]2\sigma^\kappa_{11}\\ &+\left(-\sqrt{2-2y}\,(2-y)\right)4\sigma^\kappa_{10}\cos(\phi_\ell-\phi_k) + (2(1-y))2\sigma^\kappa_{-11}\cos(2(\phi_\ell-\phi_k))\Big]\,,\end{aligned} \tag{63}$$

Table 2: Calculations of $\widetilde{X}_\kappa^{\lambda\bar{\lambda}}/(N_c^2-1)$ for various states κ. Note the off-diagonal elements vanish in collinear factorization.

	$\kappa = {}^1S_0^{[8]}$			$\kappa = {}^3S_1^{[8]}$		
	$\bar{\lambda}=0$	$\bar{\lambda}=+1$	$\bar{\lambda}=-1$	$\bar{\lambda}=0$	$\bar{\lambda}=+1$	$\bar{\lambda}=-1$
$\lambda=0$	0	0	0	0	0	0
$\lambda=+1$	0	$\frac{4e^2g^2}{M}$	0	0	0	0
$\lambda=-1$	0	0	$\frac{4e^2g^2}{M}$	0	0	0
	$\kappa = {}^3P_0^{[8]}$			$\kappa = {}^3P_1^{[8]}$		
	$\bar{\lambda}=0$	$\bar{\lambda}=+1$	$\bar{\lambda}=-1$	$\bar{\lambda}=0$	$\bar{\lambda}=+1$	$\bar{\lambda}=-1$
$\lambda=0$	0	0	0	$\frac{64e^2g^2Q^2}{3M(M^2+Q^2)^2}$	0	0
$\lambda=+1$	0	$\frac{16e^2g^2(3M^2+Q^2)^2}{3M^3(M^2+Q^2)^2}$	0	0	$\frac{32e^2g^2Q^4}{3M^3(M^2+Q^2)^2}$	0
$\lambda=-1$	0	0	$\frac{16e^2g^2(3M^2+Q^2)^2}{3M^3(M^2+Q^2)^2}$	0	0	$\frac{32e^2g^2Q^4}{3M^3(M^2+Q^2)^2}$
	$\kappa = {}^3P_2^{[8]}$					
	$\bar{\lambda}=0$	$\bar{\lambda}=+1$	$\bar{\lambda}=-1$			
$\lambda=0$	$\frac{64e^2g^2Q^2}{5M(M^2+Q^2)^2}$	0	0			
$\lambda=+1$	0	$\frac{32e^2g^2(6M^4+Q^4)}{15M^3(M^2+Q^2)^2}$	0			
$\lambda=-1$	0	0	$\frac{32e^2g^2(6M^4+Q^4)}{15M^3(M^2+Q^2)^2}$			

where we defined the density matrix for the short distance coefficients for the cross section for $\gamma^* + p \to H + X$ production as

$$\hat{\sigma}_{\lambda\bar{\lambda}}^{\kappa} = \mathrm{PDF}_g(x_g) \sum_\kappa \frac{\pi \widetilde{X}_{\lambda\bar{\lambda}}^{\kappa}}{(Q^2+M^2)^2}\,. \tag{64}$$

Using the results in Table 2, we find the following results for the short-distance coefficients:

$$\frac{\mathrm{d}\hat{\sigma}_{^1S_0}}{\mathrm{d}y\mathrm{d}Q^2\mathrm{d}\phi_{\ell k}} = \frac{\alpha_{\mathrm{em}}^2\alpha_{\mathrm{s}}\pi}{yQ^2(N_c^2-1)}\left[1+(1-y)^2\right]\frac{8}{M(Q^2+M^2)^2}\,\mathrm{PDF}_g(g)$$

$$\frac{\mathrm{d}\hat{\sigma}_{^3S_1}}{\mathrm{d}y\mathrm{d}Q^2\mathrm{d}\phi_{\ell k}} = 0$$

$$\frac{\mathrm{d}\hat{\sigma}_{^3P_0}}{\mathrm{d}y\mathrm{d}Q^2\mathrm{d}\phi_{\ell k}} = \frac{\alpha_{\mathrm{em}}^2\alpha_{\mathrm{s}}\pi}{yQ^2(N_c^2-1)}\left[1+(1-y)^2\right]\frac{32(3M^2+Q^2)^2}{3M^3(M^2+Q^2)^4}\mathrm{PDF}_g(g) \tag{65}$$

$$\frac{\mathrm{d}\hat{\sigma}_{^3P_1}}{\mathrm{d}y\mathrm{d}Q^2\mathrm{d}\phi_{\ell k}} = \frac{\alpha_{\mathrm{em}}^2\alpha_{\mathrm{s}}\pi}{yQ^2(N_c^2-1)}\Big[(1-y)\frac{256Q^2}{3M(M^2+Q^2)^4}+\left[1+(1-y)^2\right]\frac{64Q^4}{3M^3(M^2+Q^2)^2}\Big]\mathrm{PDF}_g(g)$$

$$\frac{\mathrm{d}\hat{\sigma}_{^3P_2}}{\mathrm{d}y\mathrm{d}Q^2\mathrm{d}\phi_{\ell k}} = \frac{\alpha_{\mathrm{em}}^2\alpha_{\mathrm{s}}\pi}{yQ^2(N_c^2-1)}\Big[(1-y)\frac{256Q^2}{5M(M^2+Q^2)^2}+\left[1+(1-y)^2\right]\frac{64(6M^4+Q^4)}{15M^3(M^2+Q^2)^2}\Big]\mathrm{PDF}_g(g)$$

Plugging equations (65) into Eq. (62), we find that the final expression for the differential cross-section for quarkonium production in DIS in collinear factorization is:

$$\frac{\mathrm{d}\sigma\left(p(P)+e(\ell)\to H(k)+e(\ell')+X\right)}{\mathrm{d}y\mathrm{d}Q^2\mathrm{d}\phi_{\ell k}} =$$
$$\frac{\alpha_{\mathrm{em}}^2\alpha_{\mathrm{s}}\pi}{yQ^2(N_c^2-1)}\mathrm{PDF}_g(x_g)\Bigg\{\frac{256Q^2(1-y)}{3M(M^2+Q^2)^4}\left[\langle\mathcal{O}^{J/\psi}_{^3P_1^{[8]}}\rangle+\frac{3}{5}\langle\mathcal{O}^{J/\psi}_{^3P_2^{[8]}}\rangle\right]+\frac{8\left[1+(1-y)^2\right]}{M(Q^2+M^2)^2}\Bigg\{\langle\mathcal{O}^{J/\psi}_{^1S_0^{[8]}}\rangle+$$
$$\frac{4}{3M^3(M^2+Q^2)^2}\left[(3M^2+Q^2)^2\langle\mathcal{O}^{J/\psi}_{^3P_0^{[8]}}\rangle+2Q^4\langle\mathcal{O}^{J/\psi}_{^3P_1^{[8]}}\rangle+\frac{2}{5}(6M^4+Q^4)\langle\mathcal{O}^{J/\psi}_{^3P_1^{[8]}}\rangle\right]\Bigg\}\Bigg\}. \tag{66}$$

A similar result has been obtained in [10], where they compute quarkonium production in TMD factorization. We have verified Eq. (66) can be obtained from the results in [10] after one integrates over the transverse momentum of the quarkonium, and using the relation

$$\int \mathrm{d}^2\boldsymbol{k}_\perp \mathrm{TMDPDF}_g(x_g,\boldsymbol{k}_\perp)=\mathrm{PDF}_g(x_g) \tag{67}$$

where $\mathrm{TMDPDF}_g(x_g,\boldsymbol{k}_\perp)$ is the transverse-momentum dependent gluon distribution function.

3 Future Work and Open Problems

3.1 TMD factorization

In Sect. 2.4 we assumed that each parton moves collinearly to the proton. This collinear factorization neglects the transverse motion of partons which is important for the potential angular correlations between the electron, and the quarkonium and its decay products. In future work, we will use transverse-momentum dependent factorization by means of a transverse-momentum-dependent parton distribution function $\mathrm{TMDPDF}_f(x,\boldsymbol{k}_\perp)$ which gives the probability density to find a parton f carrying longitudinal momentum fraction x and transverse momentum $\boldsymbol{k}_\perp$ inside the proton. TMD factorization is valid when another large scale in the hadronic process is much larger than $\boldsymbol{k}_\perp^2$, e.g. $Q^2 \gg \boldsymbol{k}_\perp^2$. In this case, one can neglect the $\boldsymbol{k}_\perp^2$ dependence of the partonic scattering, so that we can reuse some of the results derived in this project.

For quarks, this simply involves modifying Eq. (1) by replacing $\mathrm{PDF}_f(x)$ by $\mathrm{TMDPDF}_f(x,\boldsymbol{k}_\perp)$ and integrating over $\boldsymbol{k}_\perp$. However, for processes involving gluons the factorization is more intricate, and involves decomposing the hadron tensor in TMD factorization to include unpolarized and linearly polarized pieces.

Including TMD factorization enables us to study gluons having different polarizations in the amplitude and conjugate amplitude, similarly to the photon. Coupled with examining the decay products of the quarkonium, this will unlock additional potential angular correlations. We hope to implement this in the coming weeks.

3.2 Relativistic Corrections

We also plan to extend NRQCD calculations with relativistic corrections to improve our accuracy beyond first order computations. This novel technique hasn't been implemented in semi-inclusive DIS processes yet, and there is much to discover.

3.3 CGC formalism Implementations

Lastly, we plan to implement the Color-Glass-Condensate (CGC) effective field theory to obtain the short distance coefficients more accurately by considering coherent multiple interactions of the heavy quark pair with the proton on all orders. The CGC framework also enables us to compute DIS involving heavy nuclei more precisely. Initial steps towards this direction have been considered in [3].

Acknowledgements

I would like to thank my mentor, Professor Farid Salazar, for his continuous support, thoughtful explanations, and for sharing with me his passion for this research. I would also like to thank everyone involved in the INTURN program for providing me with this unique and exciting, supportive introduction to careers in nuclear theory. This research was supported by the INT's U.S. Department of Energy grant No. DE-FG02-00ER41132.

References

[1] A. Accardi et al. "Electron Ion Collider: The Next QCD Frontier: Understanding the glue that binds us all". In: *Eur. Phys. J. A* 52.9 (2016). Ed. by A. Deshpande, Z. E. Meziani, and J. W. Qiu, p. 268. DOI: 10.1140/epja/i2016-16268-9. arXiv: 1212.1701 [nucl-ex].

[2] Heikki Mäntysaari et al. "Gluon imaging using azimuthal correlations in diffractive scattering at the Electron-Ion Collider". In: *Phys. Rev. D* 103.9 (2021), p. 094026. DOI: 10.1103/PhysRevD.103.094026. arXiv: 2011.02464 [hep-ph].

[3] Vincent Cheung et al. "Direct quarkonium production in DIS from a joint CGC and NRQCD framework". In: (Sept. 2024). arXiv: 2409.04080 [hep-ph].

[4] Michael E. Peskin and Daniel V. Schroeder. *An Introduction to quantum field theory*. Reading, USA: Addison-Wesley, 1995. ISBN: 978-0-201-50397-5, 978-0-429-50355-9, 978-0-429-49417-8. DOI: 10.1201/9780429503559.

[5] Renaud Boussarie et al. "TMD Handbook". In: (Apr. 2023). arXiv: 2304.03302 [hep-ph].

[6] Astrid Morreale and Farid Salazar. "Mining for Gluon Saturation at Colliders". In: *Universe* 7.8 (2021), p. 312. DOI: 10.3390/universe7080312. arXiv: 2108.08254 [hep-ph].

[7] F. D. Aaron et al. "Combined Measurement and QCD Analysis of the Inclusive e+- p Scattering Cross Sections at HERA". In: *JHEP* 01 (2010), p. 109. DOI: 10.1007/JHEP01(2010)109. arXiv: 0911.0884 [hep-ex].

[8] Geoffrey T. Bodwin, Eric Braaten, and G. Peter Lepage. "Rigorous QCD analysis of inclusive annihilation and production of heavy quarkonium". In: *Phys. Rev. D* 51 (1995). [Erratum: Phys.Rev.D 55, 5853 (1997)], pp. 1125–1171. DOI: 10.1103/PhysRevD.55.5853. arXiv: hep-ph/9407339.

[9] Mathias Butenschoen and Bernd A. Kniehl. "production in NRQCD: A global analysis of yield and polarization". In: *Nuclear Physics B - Proceedings Supplements* 222–224 (Jan. 2012), pp. 151–161. ISSN: 0920-5632. DOI: 10.1016/j.nuclphysbps.2012.03.016. URL: http://dx.doi.org/10.1016/j.nuclphysbps.2012.03.016.

[10] Alessandro Bacchetta et al. "Gluon TMDs and NRQCD matrix elements in J/ψ production at an EIC". In: *Eur. Phys. J. C* 80.1 (2020), p. 72. DOI: 10.1140/epjc/s10052-020-7620-8. arXiv: 1809.02056 [hep-ph].